

Design of Rectangular Openings in Precast Walls Under Vertical Loads



Michael G. Allen

Designer
Degenkolb Engineers
San Francisco, California
(Former Graduate Research Assistant,
Civil Engineering and Geological
Sciences, University of Notre Dame,
Notre Dame, Indiana)

One of the successful precast concrete systems that has emerged from the PRESSS (PREcast Seismic Structural Systems) research program is the unbonded post-tensioned concrete wall system. This paper addresses the use of these walls with rectangular openings to accommodate architectural, mechanical, and safety requirements. The openings can cause large tensile stresses and, thus, cracking in the wall panels. Little information is available to aid in the design of the panel reinforcement around the openings to limit the size of these cracks. This paper describes an analytical investigation of the behavior and design of the walls under vertical post-tensioning and gravity loads. Critical regions in the wall panels where bonded mild steel reinforcement is needed are identified and a design approach is proposed to determine the required panel reinforcement. The effects of opening length, opening height, wall length, and initial stress in the concrete due to post-tensioning and gravity loads are considered. An example is included to demonstrate the proposed design approach.



Yahya C. Kurama, Ph.D.

Assistant Professor
Civil Engineering and
Geological Sciences
University of Notre Dame
Notre Dame, Indiana

Research conducted as a part of the PRESSS (PREcast Seismic Structural Systems) research program has shown that precast concrete walls with unbonded post-tensioning offer significant advantages as primary lateral load-resisting systems in seismic regions.¹⁻⁴ Fig. 1 shows the elevation and cross section near the base of a wall, referred to as Wall WH1M, which was designed for a region with high seismicity (e.g., coastal California) and a site with a “medium”

soil profile [a soil profile with deep cohesiveness or stiff clay conditions where the soil depth exceeds 200 ft (61 m)].

The wall is constructed by post-tensioning precast wall panels across horizontal joints using high strength bars that are not bonded to the concrete. Dry-pack or grout may be used between the wall panels to keep them within construction and alignment tolerances. Spiral reinforcing steel is used to confine the concrete near the base of

the wall. Welded wire fabric is used as bonded reinforcement in the panels.

The post-tensioning steel bars are anchored to the wall at the foundation and roof. Unbonding of the post-tensioning steel, which is achieved by placing the bars inside oversized ungrouted ducts, has two important advantages under lateral loads:¹

1. It results in a uniform strain distribution in the steel and, thus, delays nonlinear straining (i.e., yielding) of the post-tensioning bars.

2. It significantly reduces the tensile stresses in the concrete, and thus reduces cracking, because the stress transfer between the steel and the concrete due to bond is eliminated.

Previous research on the seismic behavior and design of unbonded post-tensioned precast concrete walls is limited to walls without openings. The use of openings in the walls, however, may be needed to accommodate windows, doors, and mechanical penetrations. Large panel openings may also be necessary in precast concrete parking structures to provide passive security protection.

The seismic design of Wall WH1M was done for a prototype structure described in Kurama et al.¹ using a design procedure developed previously for walls without openings. This design procedure, which is described in detail by Kurama et al.,^{1,3} was used to determine the wall length and thickness as well as the required amount of post-tensioning and spiral reinforcement.

The openings in the wall panels are not addressed by the previous design approach. These openings can result in large tensile stresses and, thus, cracking in the panels, which can limit the vertical and lateral load-carrying capacity of the walls by causing premature failure of the panels. Thus, bonded mild steel reinforcement may be needed in the wall panels to limit the size of the cracks.

This paper addresses the design of the required panel reinforcement around the openings under post-tensioning and gravity loads only. The research, conducted as part of a Daniel P. Jenny Research Fellowship funded by the Precast/Prestressed Concrete Institute, is described in detail by Allen and Kurama.⁵

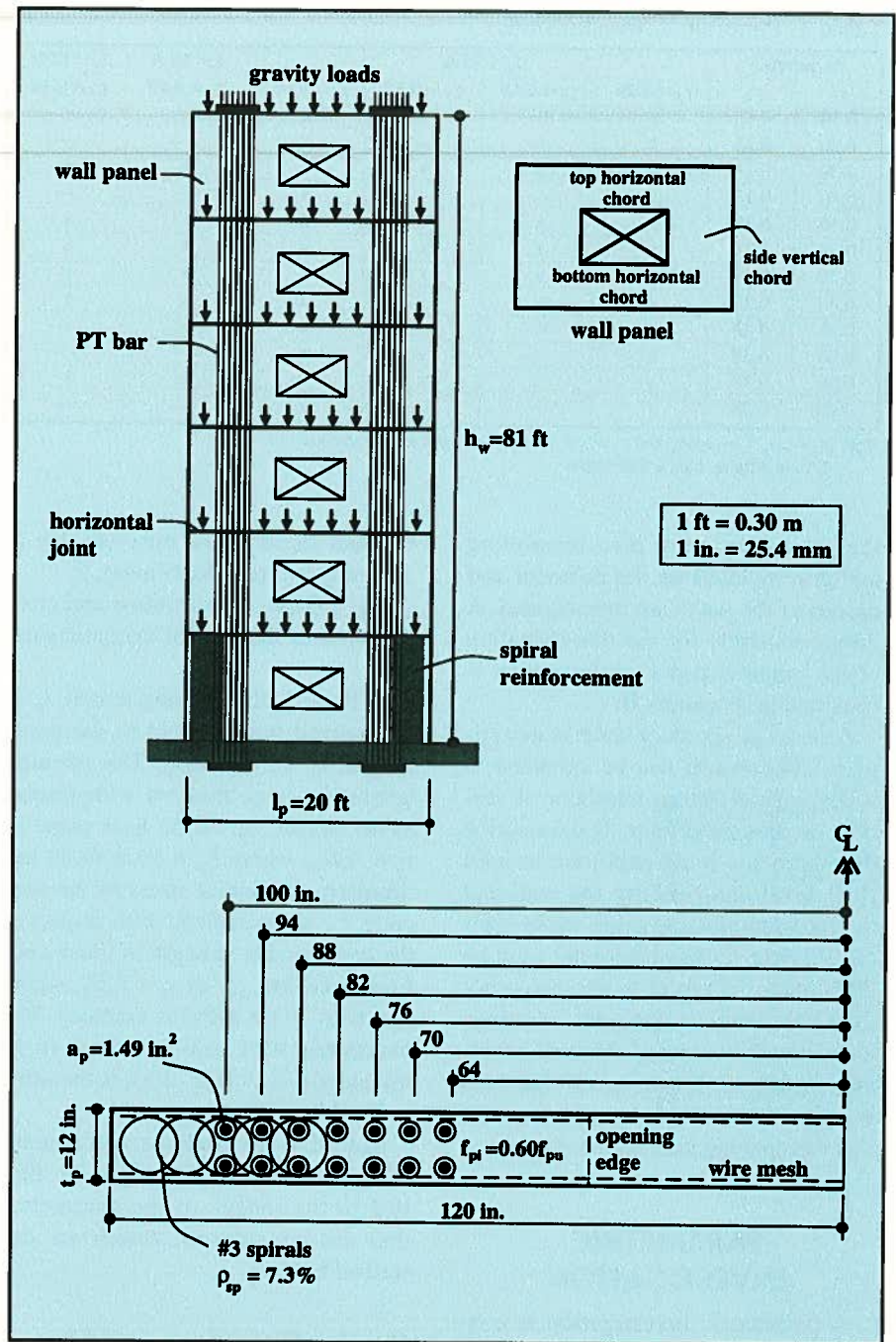


Fig. 1. Prototype Wall WH1M: elevation and cross section (half the wall length).

OBJECTIVES AND SCOPE

The research project focuses on two stages of loading for the walls. In the first stage, the walls are subjected only to vertical post-tensioning forces and gravity loads. This is the loading stage that a typical wall would be subjected to during most of its service life. The second stage of loading is the combination of vertical loads with lateral loads, such as earthquakes.

The behavior and design of the walls for the first stage of loading is

discussed in this paper. The second stage of loading is addressed in Allen and Kurama,⁶ to be published in the March-April 2002 PCI JOURNAL. For each loading stage, the critical regions in the wall panels are identified and a design approach to determine the required amount of bonded panel reinforcement to control cracking and prevent premature failure of the walls is proposed.

The effects of opening length and height, wall length, and initial stress in

Table 1. Parametric investigation.

Parameter		$l_p = 20$ ft				$l_p = 15$ ft	$l_p = 12$ ft
γ_l	γ_h	$\gamma_f = 0.29$	$\gamma_f = 0.18$	$\gamma_f = 0.11$	$\gamma_f = 0.057$	$\gamma_f = 0.18$	$\gamma_f = 0.18$
0.10	0.13	x	—	—	x	—	—
0.20	0.13	x	—	—	x	—	—
0.30	0.13	x	x	x	x	x	x
0.40	0.13	x	—	—	x	—	—
0.10	0.25	x	x	x	x	x	x
0.20	0.25	x	x	x	x	x	x
0.30	0.25	x	x	x	x	x	x
0.40	0.25	x	x	x	x	x	x
0.10	0.38	x	—	—	x	—	—
0.20	0.38	x	—	—	x	—	—
0.30	0.38	x	x	x	x	x	x
0.40	0.38	x	—	—	x	—	—

Note: $\gamma_l = l_o/l_p$, $\gamma_h = h_o/h_p$, and $\gamma_f = f_{ci}/f'_c$, where $h_p = 16$ ft and $f'_c = 6.0$ ksi. 1 ft = 0.3048 m, 1 ksi = 6.895 MPa.

the concrete due to post-tensioning and gravity loads on the behavior and design of the walls are investigated. A design example for the determination of the required panel reinforcement is provided in Appendix B.

A series of six-story walls is investigated. The results can be extended to walls with different numbers of stories, as described later. It is assumed that there is a horizontal joint at each floor level and between the wall and the foundation since larger panel sizes (with fewer horizontal joints) may be difficult to transport to the construction site. Only rectangular openings located at the center of the wall panels are considered. It is assumed that each story panel contains an opening and that the opening size does not vary.

PARAMETRIC INVESTIGATION

A parametric investigation is conducted on walls with openings using a finite element model that is described later. The objectives of the parametric investigation are to:

- Determine the effect of the openings on the behavior of the walls.
- Determine the critical regions in the wall panels and the required amount of bonded panel reinforcement in these regions.
- Develop an approach for designing the panel reinforcement.

Table 1 shows the parameters that are investigated; these are:

- Opening length, l_o
- Opening height, h_o
- Panel (wall) length, l_p

- Initial stress in the concrete due to gravity and post-tensioning, f_{ci}

Fig. 2 shows the elevation and cross section near the base of the parametric walls.

In Table 1, the opening length, l_o , is normalized with respect to the panel length, l_p , as $\gamma_l = l_o/l_p$. The opening height, h_o , is normalized with respect to the height, h_p , of the base panel as $\gamma_h = h_o/h_p$, where $h_p = 16$ ft (4.88 m). Similarly, the initial stress in the concrete, f_{ci} , is normalized with respect to the compressive strength of the unconfined concrete, f'_c , as $\gamma_f = f_{ci}/f'_c$, where $f'_c = 6$ ksi (41.4 MPa) is assumed. The parametric wall with $l_p = 20$ ft (6.10 m) and $\gamma_f = 0.29$ [Fig. 2(a)] is the same as Wall WH1M (see Fig. 1).

Note that the findings and conclusions presented in this paper are limited to the ranges of the parameters that are considered, which are described below.

Opening Dimensions, l_o and h_o

As shown in Table 1, the parametric investigation of the normalized opening dimensions is limited to $0.10 \leq \gamma_l \leq 0.40$ and $0.13 \leq \gamma_h \leq 0.38$. The maximum length of the openings is limited so that the post-tensioning bars can be placed within the vertical chords at the sides of the openings (see Fig. 1). (The placement of the bars inside the openings is considered unsafe.)

Moreover, under combined vertical and lateral loads, all or most of the axial forces in a wall (due to gravity and post-tensioning) are transferred to the foundation through the vertical chord at the compression side of the

base panel (as described in more detail by Allen and Kurama^{5,6}). The maximum length and height of the openings are limited to ensure that the wall panels remain stable under these large compression forces.

For openings that are larger than those investigated in this paper, it may be necessary to brace the openings to stabilize the wall panels under combined vertical and lateral loads. The presence of larger openings may also necessitate that the walls be designed as either coupled wall systems or frame systems.

Panel Dimensions, l_p , h_p , and t_p

The parametric investigation of the panel (wall) length is limited to 12 ft (3.66 m) $\leq l_p \leq 20$ ft (6.10 m) as shown in Table 1 and Fig. 2. The panel height, h_p , is assumed to be equal to 16 ft (4.88 m) for the base panel and 13 ft (3.96 m) for the upper story panels. The panel thickness, t_p , is kept constant at 12 in. (305 mm).

The maximum size and weight of the panels are limited to ensure that the panels can be transported to the construction site. The shorter panel lengths considered in the paper can be used in wall systems with vertical joints, similar to the walls investigated by Priestley et al.,⁴ Kurama,⁷ and Perez.⁸

Initial Concrete Stress, f_{ci}

The initial stress in the concrete is calculated as a nominal initial stress, by dividing the axial force near the base of the wall with the gross cross-sectional area, $A_g = l_p t_p$. The parametric investigation of the normalized initial concrete stress due to post-tensioning and gravity loads is limited to $0.057 \leq \gamma_f \leq 0.29$.

The total initial (i.e., after losses) post-tensioning force in the walls is calculated as $P_i = \sum a_p f_{pi}$, where a_p is the area of a post-tensioning bar and f_{pi} is the initial stress in the bar. The variation in the initial concrete stress is achieved by varying the total area of the post-tensioning steel as shown in Fig. 2 to represent walls designed for different levels of seismicity.

The normalized initial concrete

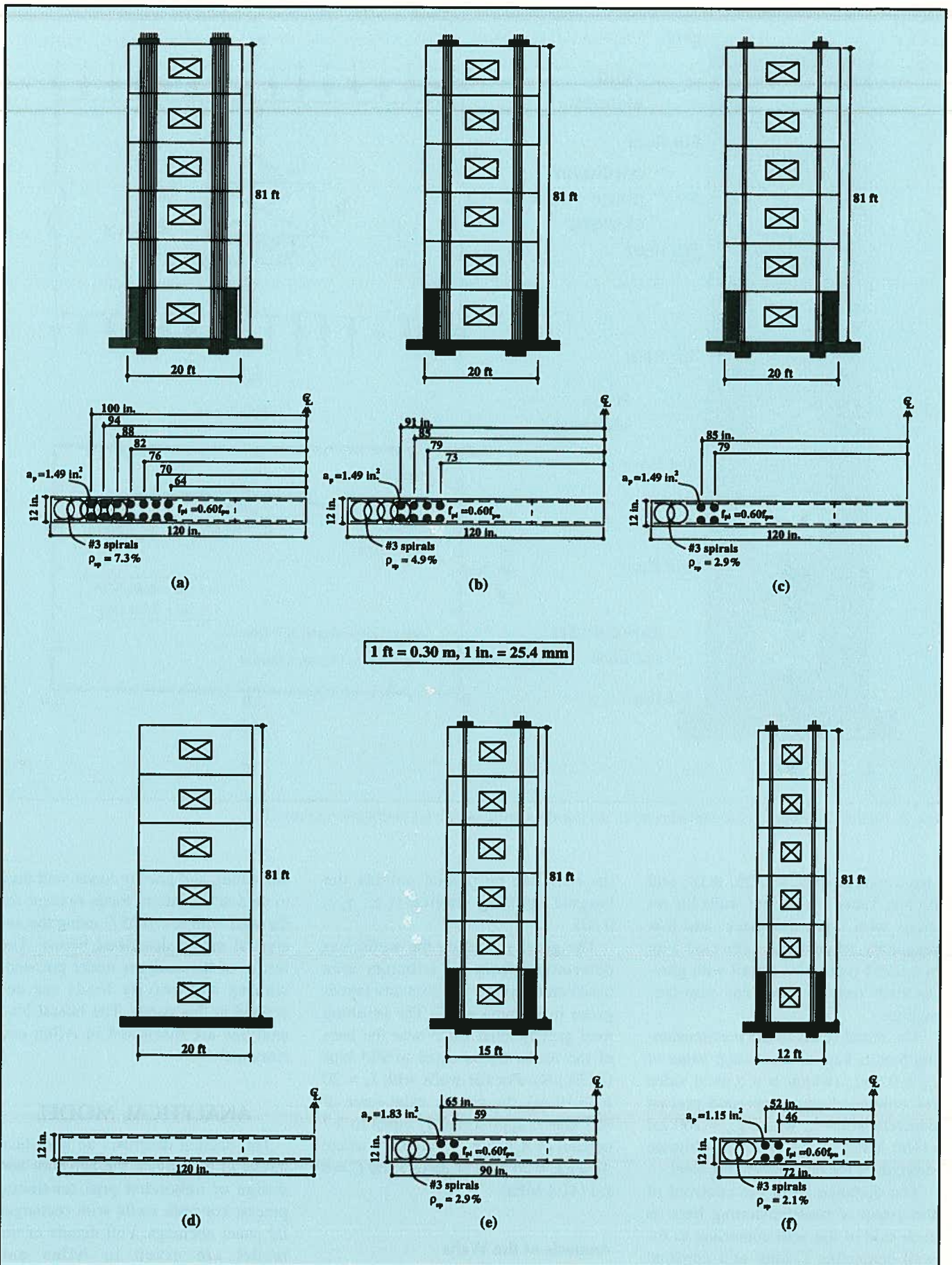


Fig. 2. Elevation and cross section of the parametric walls: (a) $l_p = 20$ ft, $\gamma_f = 0.29$; (b) $l_p = 20$ ft, $\gamma_f = 0.18$; (c) $l_p = 20$ ft, $\gamma_f = 0.11$; (d) $l_p = 20$ ft, $\gamma_f = 0.057$; (e) $l_p = 15$ ft, $\gamma_f = 0.18$; (f) $l_p = 12$ ft, $\gamma_f = 0.18$.

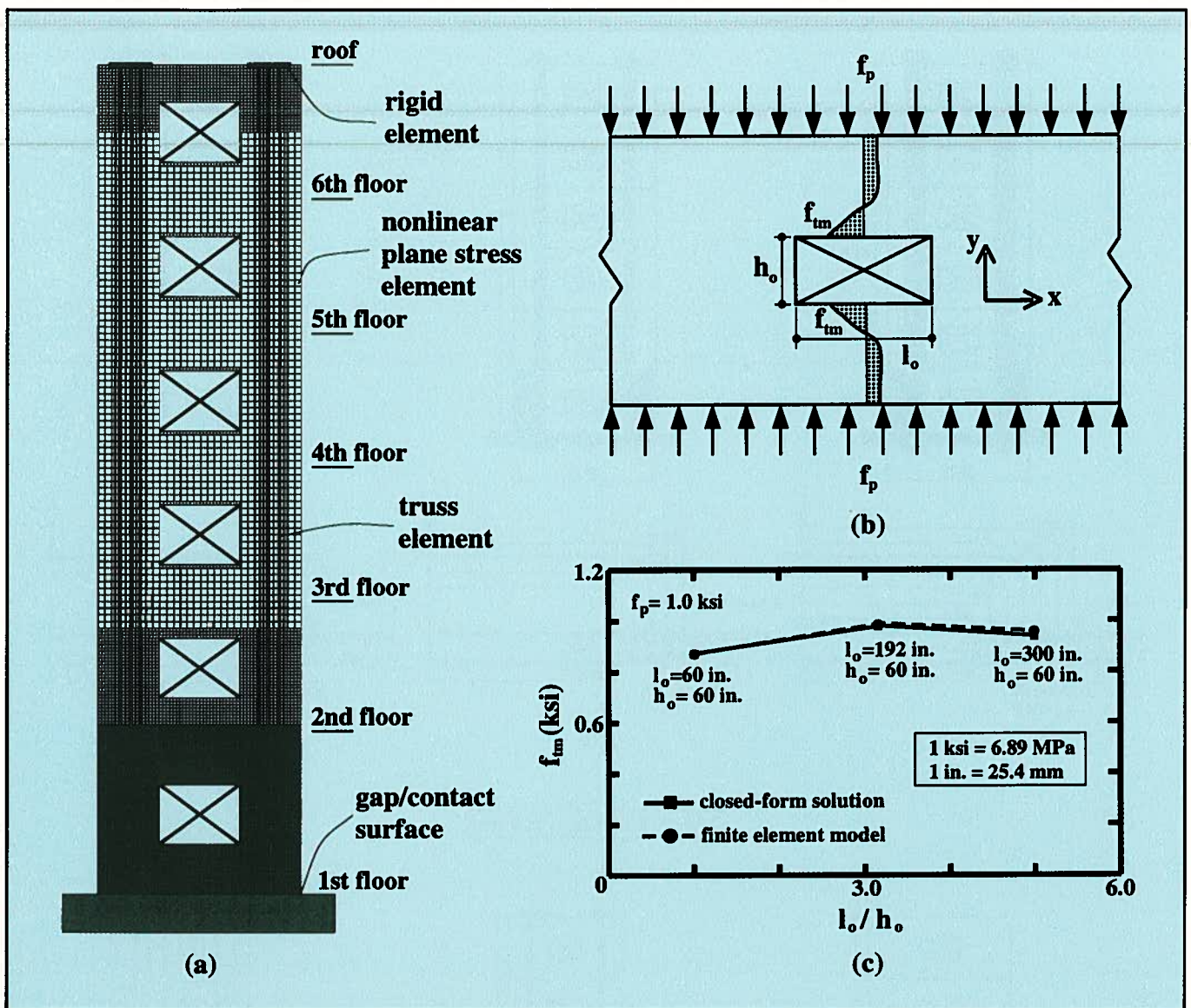


Fig. 3. Analytical model: (a) model elevation; (b) infinite elastic panel; (c) verification of results.

stress values of $\gamma_f = 0.29, 0.18,$ and 0.11 in Table 1 represent walls for regions with high, moderate, and low seismicity, respectively. The case with $\gamma_f = 0.057$ represents a wall with gravity loads only, without any post-tensioning.

The initial stress in the post-tensioning bars is kept at a constant value of $f_{pi} = 0.60f_{pu}$ (which is a typical value for unbonded post-tensioned precast concrete walls^{1,2}), where $f_{pu} = 160$ ksi (1100 MPa) is the assumed ultimate strength of the post-tensioning steel.

The distance from the centroid of the group of post-tensioning bars on each side of the wall centerline to the wall centerline is kept at a constant proportion (34.1 percent) of the wall length. This location is selected so that

the bars can be placed outside the longest opening studied (i.e., $\gamma_l = 0.40$).

The gravity load on the walls was determined from the tributary area based on the prototype structure layout given in Kurama et al.¹ The resulting total gravity axial force near the base of the walls, G_b , is equal to 983 kips (4370 kN). For the walls with $l_p = 20$ ft (6.10 m), the gravity axial force of 983 kips is approximately equal to 5.7 percent of $A_g f'_c$ (i.e., $\gamma_f = 0.057$), where $A_g = l_p t_p = 20$ sq ft (1.86 m²) and $f'_c = 6$ ksi (41.4 MPa).

Analysis of the Walls

In the parametric investigation, each wall is first subjected to post-

tensioning and gravity loads, and then to equivalent lateral loads (except for the wall with $\gamma_f = 0.057$) using the analytical model described below. The results of the analyses under post-tensioning and gravity loads are described in this paper. The lateral load analyses are discussed in Allen and Kurama.⁶

ANALYTICAL MODEL

This section describes an analytical model to investigate the behavior and design of unbonded post-tensioned precast concrete walls with rectangular panel openings. Full details of the model are given in Allen and Kurama.⁵

As an example, Fig. 3(a) shows the

analytical model for Wall WH1M. The model, which was developed using the finite element program ABAQUS,⁹ can be used to conduct nonlinear analyses of walls with and without openings under vertical and lateral loads.

Modeling of the post-tensioning bars, wall panels, and gravity loads is described below. Modeling of the behavior of the walls under lateral loads is described in Allen and Kurama.^{5,6}

Modeling of Post-Tensioning Bars

The unbonded post-tensioning bars are modeled using truss elements. The post-tensioning anchors at the foundation are represented by restraining the vertical and horizontal translational degrees of freedom of the truss element nodes located at the foundation level. The post-tensioning anchors at the roof level are modeled using rigid elements that share nodes with elements modeling the wall panels (described below).

The post-tensioning loads are simulated by initial tensile forces in the truss elements, which are equilibrated with compression stresses in the wall panels. The "smooth" stress-strain relationship of the post-tensioning steel in tension is modeled using an idealized tri-linear stress-strain relationship.⁵

The yield stress of the tri-linear relationship is determined from the linear limit (i.e., limit of proportionality) stress of the smooth stress-strain relationship as $f_{py} = 120$ ksi (827 MPa). The strain-hardening stiffness is determined from the nonlinear portion of the smooth stress-strain relationship up to the ultimate strength, $f_{pu} = 160$ ksi (1103 MPa).

Modeling of Wall Panels and Gravity Loads

The precast concrete wall panels are modeled using nonlinear rectangular plane stress elements. It is assumed that the panels remain stable under the applied loads. The gravity loads are modeled as uniformly distributed loads applied to the top of the panels at each floor and roof level.

A series of mesh refinement analyses were conducted to determine the

finite element mesh.⁵ As shown in Fig. 3(a), a large number of elements are used to model the wall panels. The number of elements is increased at the top of the wall near the post-tensioning anchors and in the base panel, which is the most critical panel due to larger stresses. The size of each element in the base panel is 2 x 2 in. (50.8 x 50.8 mm). The openings are modeled by regions in the wall panels without any elements.

The spiral reinforcing steel in the wall panels is not modeled explicitly. Instead, the effect of the spiral reinforcement is represented using a confined concrete stress-strain relationship in the elements modeling the wall panels as described in detail by Allen and Kurama.⁵ The nonlinear compressive stress-strain relationships of the unconfined concrete and the spiral confined concrete are determined using a model developed by Mander et al.¹⁰

Variations in the concrete properties across the thickness of the wall panels (such as cover concrete) are ignored to reduce the size of the analytical model and to prevent numerical problems due to the crushing of the cover concrete under lateral loads. Previous investigations of walls without openings have shown that crushing of the cover concrete under lateral loads occurs over a small region near the bottom corners of the base panel and does not have a significant effect on the behavior of the walls.³ Thus, crushing of the cover concrete is not modeled in this study. The reduction in the concrete area due to the post-tensioning ducts is also not modeled.

Modeling of Bonded Panel Reinforcement

The bonded panel reinforcement, which includes the mild steel reinforcement needed around the openings and the welded wire fabric, is not modeled explicitly. Since the actual amount and location of the mild steel reinforcement around the openings is not known in advance, an explicit modeling of this reinforcement would necessitate an iterative analysis procedure to determine the required area, number, and location of the bars using

an accurate representation of each bar in the wall panels. This iterative procedure would significantly limit the number of walls that could be investigated by the research because of an increased number of analyses necessary for each wall, difficulties in the modeling of individual bars and cracking of concrete, numerical problems, and execution time.

These difficulties are overcome by modeling the effect of the bonded steel reinforcement using elastic tension properties in the plane stress elements for the wall panels. In this modeling approach, the following assumptions are made:

- The panels are reinforced with a sufficient amount of bonded mild steel to limit the size of the cracks.
- The panel reinforcement does not yield.
- The reinforcement is well-distributed and well-detailed in the tension regions.

Based on these assumptions, the required area of reinforcement can be determined from the tensile stresses in the wall panels.

Note that as a result of using elastic tension properties in the wall panels, the redistribution of panel stresses due to concrete cracking and the actual placement of the panel reinforcement cannot be modeled. However, in a properly designed panel with a sufficient amount of well-distributed, well-detailed reinforcement, the cracks remain small and, thus, are not expected to significantly affect the behavior.

Verification of the Analytical Model Under Vertical Loads

The finite element model under vertical loads is verified as described below. The verification of the model under combined vertical (due to gravity and post-tensioning) and lateral loads is described in Allen and Kurama.^{5,6}

Closed-form analytical solutions are available for the maximum tensile stresses in infinite elastic panels with rectangular openings for a limited number of load and opening configurations.^{5,11} As an example, Fig. 3(b) shows a panel loaded with a uniform compression stress, f_p .

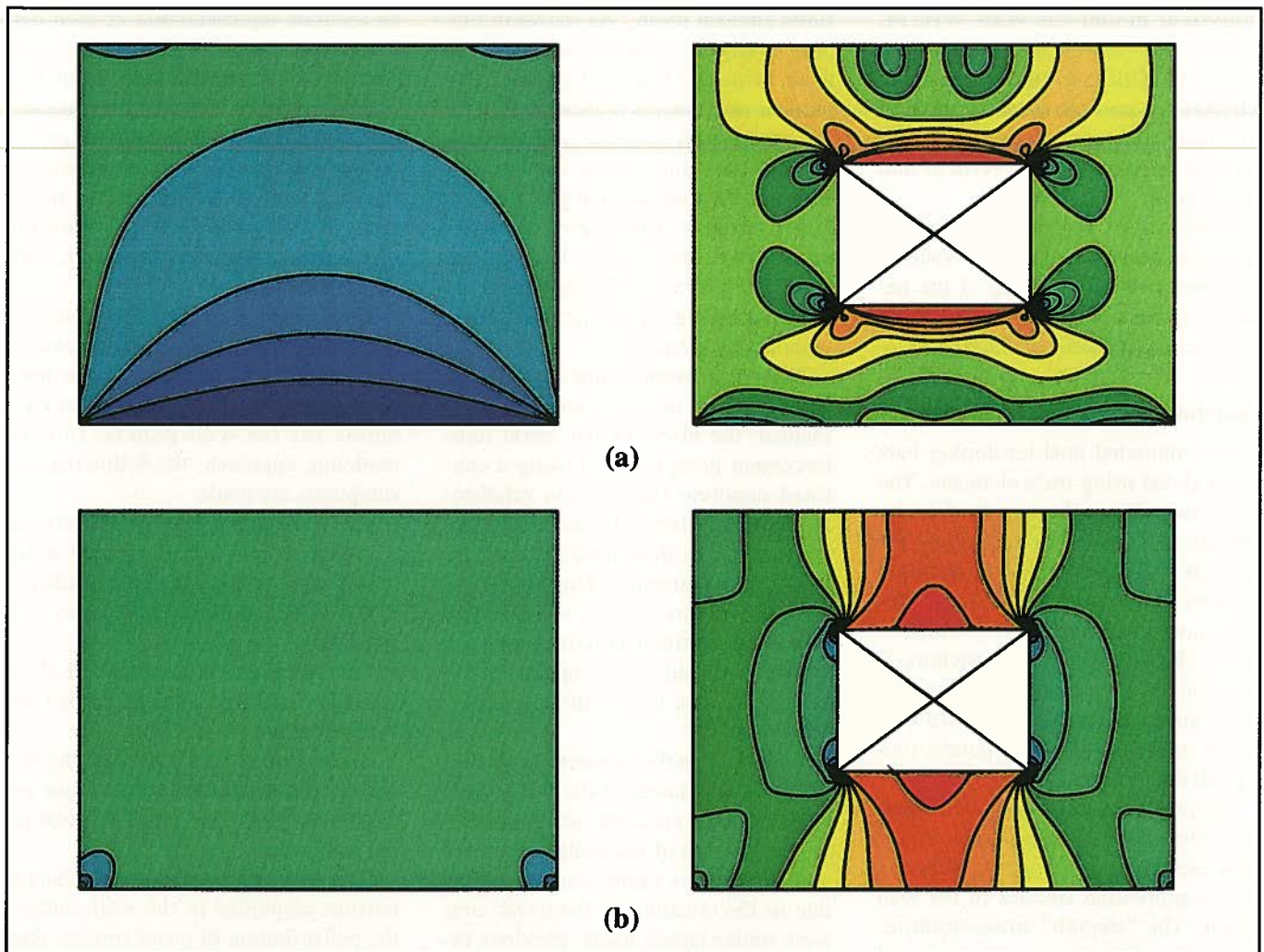


Fig. 4. Stress contours in the base panel: (a) maximum principal stresses; (b) minimum principal stresses.

This loading condition is similar to the condition that exists in the wall panels under vertical loads due to gravity and post-tensioning as described later. The presence of an opening in the panel results in the development of normal stresses (in the horizontal, x -direction) above and below the opening as shown in Fig. 3(b). The stresses near the opening are tensile, with the maximum tension stress, f_{tm} , occurring at the middle of the opening edge.

Fig. 3(c) shows comparisons between the maximum tension stress, f_{tm} , calculated using the closed-form solution and the stress predicted using a finite element model of the panel.⁵ The comparisons are provided for three different opening aspect ratios ($l_o/h_o = 1.0, 3.2, \text{ and } 5.0$) under a panel loading of $f_p = 1.0$ ksi (6.89 MPa). The results indicate that the finite element model is capable of accurately predict-

ing the maximum tension stress adjacent to the opening for different values of opening length, l_o and height, h_o .

CRITICAL PANEL REGIONS UNDER VERTICAL LOADS

As described earlier, a typical precast concrete wall with unbonded post-tensioning would primarily be subjected to vertical loads due to gravity and post-tensioning during most of its service life. Under these conditions, cracks may form in the wall panels due to the openings. To limit the size of these cracks, the most critical regions in the wall panels need to be identified and reinforced with a sufficient amount of bonded mild steel.

As an example, Fig. 4 shows the principal stress contours in the base panel of Wall WH1M [$l_p = 20$ ft (6.10 m) and $\gamma_f = 0.29$] using the finite element model. Figs. 4(a) and 4(b) show

the maximum and minimum principal stress contours, respectively, in the panel without and with an opening ($\gamma_l = 0.40$ and $\gamma_h = 0.38$).

The red-shaded areas in Fig. 4(a) indicate the critical regions of the panel where the maximum principal stresses exceed $7.5\sqrt{f'_c}$ in tension. The red-shaded areas in Fig. 4(b) show regions of the panel where the minimum principal stresses are tensile (i.e., greater than zero). The sign convention used for the stresses is positive for tension stresses. Cracking is expected to occur in the critical regions where the maximum principal stresses are larger than $7.5\sqrt{f'_c}$.

Fig. 4 shows that the presence of an opening disrupts the flow of the compressive stresses from the top to the bottom of the panel, resulting in the formation of tensile stresses. The critical panel regions under vertical loads are along the top and bottom edges of

the opening. The maximum tensile stresses form at the middle of the opening edges and may be large enough to cause cracking.

The finite element analysis results indicate that the directions of the critical principal stresses in the panel are mostly horizontal⁵ and, thus, horizontal reinforcement is needed parallel to the top and bottom edges of the opening. The stresses above and below the opening are similar; thus, similar amounts of reinforcement are needed in both regions.

As described earlier, the panels are modeled using elastic tension properties assuming that the critical regions are reinforced with an adequate amount of well-distributed bonded mild steel. Thus, the tensile stresses in the panels are allowed to exceed the cracking stress. The required area of the steel is determined by dividing the stress resultant in the tension region (which is calculated by integrating the tensile stresses) with the assumed allowable strength of the steel. The tensile strength of concrete is ignored in the design of the reinforcement.

Note that for the opening and panel sizes and loads considered in this paper, shear reinforcement is not needed in the wall panels under vertical loads. Thus, the design of the panel shear reinforcement is not addressed.

DESIGN OF PANEL REINFORCEMENT

This section investigates the required panel reinforcement above and below the openings based on the finite element analysis results of the parametric walls in Table 1. A design approach is proposed to estimate the amount of required reinforcement. For each wall, the design of the base panel is investigated in detail; this is the critical panel since the effect of the gravity loads is maximum at the base while the post-tensioning force is constant over the height of the wall.

Fig. 5(a) shows the compression stresses, σ_p , acting at the top of a typical base panel from the gravity loads applied at the second floor level [see Fig. 3(a)] and from the post-tensioning and gravity loads transferred to the panel by the panel above. These

stresses are obtained from the finite element model and are referred to as the panel top stresses. The stress distribution is shown only on the right half of the panel due to symmetry about the panel centerline.

The distribution of the stresses acting at the top of the panel is not uniform because of the presence of the openings. Note that the panel loading shown in Fig. 5(a) is similar to the loading in Fig. 3(b), except that the stress distribution in Fig. 5(a) is not uniform.

The compressive stresses, σ_s , at the top of the vertical chord on the right side of the opening are also shown in Fig. 5(a). These stresses are in equilibrium with the panel top stresses and are referred to as the side chord stresses.

Similar to Fig. 3(b), the presence of the opening results in normal stresses (in the horizontal, x -direction) in the horizontal chord above the opening. The tension stress resultant, T_v , in the chord is determined by integrating the stresses in the tension region over a height of h_{rv} as shown in Fig. 5(a). Then, the required area of the steel reinforcement, A_v , is determined by dividing the tension stress resultant, T_v , with the assumed allowable strength of the steel, f_{all} .

Truss Model

For design, the tension stress resultant, T_v , in the top horizontal chord is estimated using a "truss" model as shown in Fig. 5(b) and enlarged in Fig. 5(c). As shown in Fig. 4, the opening disturbs the flow of the compression stresses from the top to the bottom of the panel. The truss model is used to represent the flow of the stresses around the opening.

The truss model uses only a portion of the panel top stresses and the side chord stresses. The portion of the compressive stress resultant used in the truss model is referred to as C_r , which is calculated from the panel top stresses and the side chord stresses over a distance of x_r from the panel centerline as shown by the shaded areas in Fig. 5(b).

Let the location (measured from the panel centerline) of the stress resul-

tant, C_r , be equal to \bar{x}_p and \bar{x}_s at the top of the panel and at the top of the side chord, respectively. Based on the finite element analysis results, it is assumed that the location of C_r at a height of $l_p/4 \leq h_c$ [where $h_c = (h_p - h_o)/2$ is the height of the top chord as shown in Fig. 5(a)] from the top of the opening is also equal to \bar{x}_p . Thus, the design tension stress resultant above the opening, T_v , and the required area of the steel reinforcement, A_v , can be estimated as:

$$T_v = C_r \left(\frac{\bar{x}_s - \bar{x}_p}{l_p / 4} \right) \quad (1)$$

$$A_v = \frac{T_v}{f_{all}}$$

The determination of C_r , \bar{x}_p , and \bar{x}_s for use in Eq. (1) is described below.

Estimation of Panel Top Stresses

The panel top stresses are estimated by dividing the stress distribution from $x = 0$ (panel centerline) to $x = l_p/2$ (panel edge) into three regions:

- $0 \leq x \leq x_1$;
- $x_1 \leq x \leq x_2$; and
- $x_2 \leq x \leq l_p/2$

where x is the distance measured from the panel centerline. The stress distributions in these regions are expressed in terms of the stresses f_{p0} , f_{p1} , f_{p2} , and f_{pe} at $x = 0$, x_1 , x_2 , and $l_p/2$, respectively [see Fig. 5(b)].

The stress distribution in each region, σ_{pj} , is approximated using a second order curve as:

$$\sigma_{pj} = a_{pj}x^2 + b_{pj}x + c_{pj} \quad (2)$$

where the subscript j indicates the stress distribution in the j th region and a_{pj} , b_{pj} , and c_{pj} are coefficients used for each stress distribution. The stress $\sigma_{p1}(0) = f_{p0}$ at $x = 0$ is estimated as:

$$f_{p0} = \frac{f_{pa}}{45}(\theta_c - 40) + f_{pp} \quad (3)$$

The stress f_{pp} is equal to the uniformly distributed stress due to the gravity load, G_p , applied at the floor level above the panel (e.g., second floor for the base panel), and f_{pa} is equal to the uniformly distributed

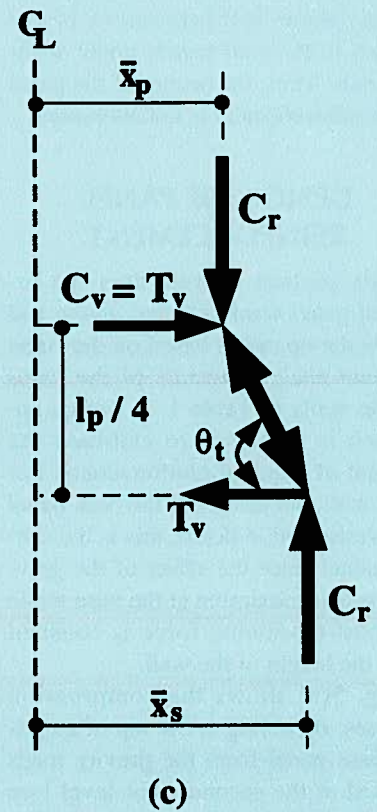
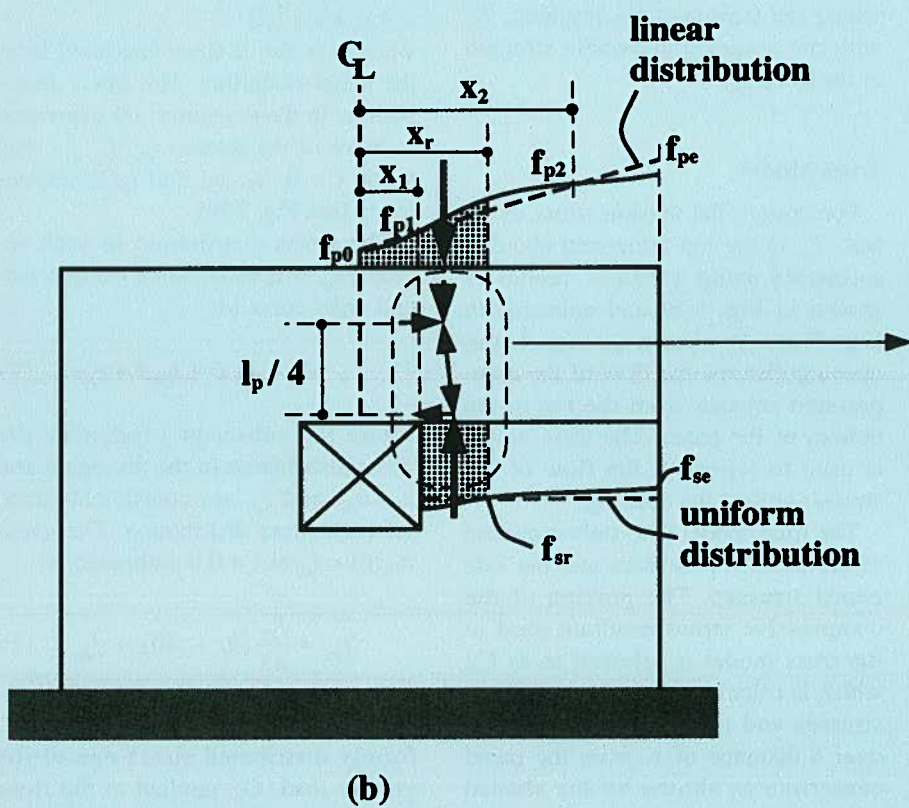
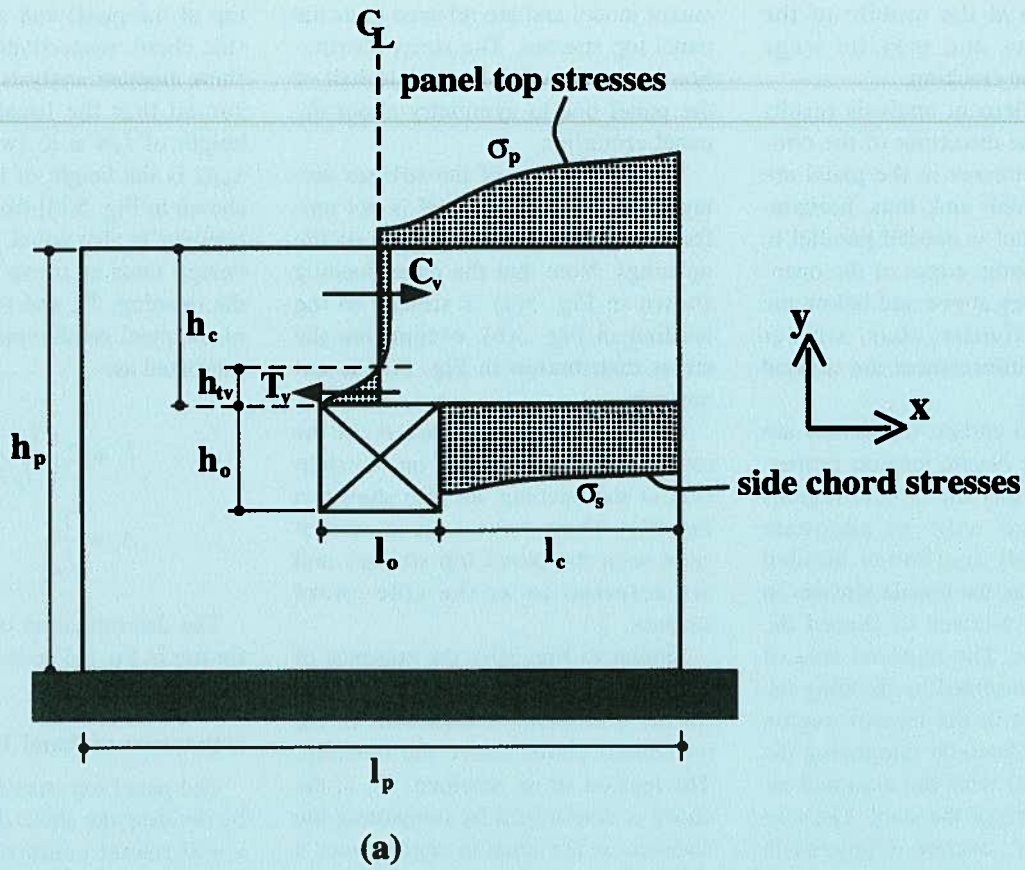


Fig. 5. Design of panel reinforcement: (a) stress distributions; (b) truss model; (c) truss model enlarged.

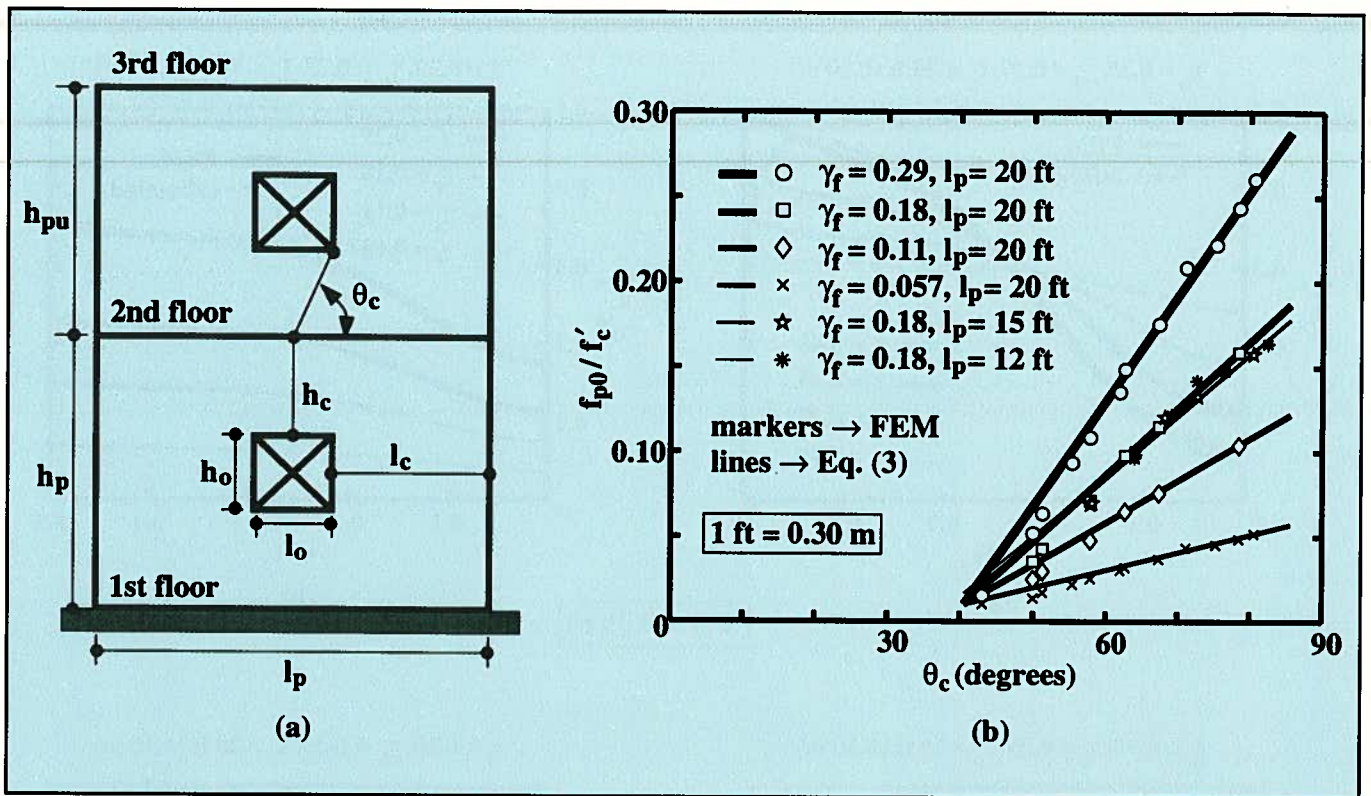


Fig. 6. Estimation of f_{p0} : (a) definition of θ_c ; (b) f_{p0} versus θ_c .

stress due to the total post-tensioning force, P_i , and the sum of the gravity loads, G_a , applied at the upper floor and roof levels (e.g., third floor and up for the base panel) as:

$$f_{pp} = \frac{G_p}{l_p t_p}$$

$$f_{pa} = \frac{P_i + G_a}{l_p t_p} \quad (4)$$

where l_p and t_p are the panel length and thickness, respectively.

The angle θ_c (in degrees) is measured between the panel centerline and the bottom corner of the opening in the upper story panel [see Fig. 6(a)] as:

$$\theta_c = \tan^{-1} \left(\frac{h_{pu} - h_o}{l_o} \right) \quad (5)$$

where h_{pu} is the height of the upper story panel (i.e., the panel above).

Fig. 6(b) shows how Eq. (3) (shown by the solid lines) compares with the f_{p0} values obtained using the finite element model (FEM, as shown by the markers) for different values of γ_l , γ_h , γ_f , and l_p . The stress f_{p0} is normalized with respect to the strength of the un-

confined concrete, $f'_c = 6$ ksi (41.4 MPa). The variation in the angle θ_c in Fig. 6(b) is a result of the variations in γ_l and γ_h .

The distances x_1 and x_2 are selected such that the stresses f_{p1} and f_{p2} (at x_1 and x_2 , respectively) can be estimated using a linear stress distribution as shown by the dashed line in Fig. 5(b). Based on the stress distributions obtained from the finite element analyses, it is assumed that:

$$x_1 = \frac{l_o}{2}$$

$$x_2 = \frac{2l_o + l_p}{4} \quad (6)$$

The stresses f_{pe} , f_{p2} , and f_{p1} for the linear stress distribution at $x = l_p/2$, x_2 , and x_1 , respectively, are determined as:

$$f_{pe} = \frac{2(P_i + G_p + G_a)}{l_p t_p} - f_{p0}$$

$$f_{p2} = f_{p0} + \frac{2(f_{pe} - f_{p0})x_2}{l_p}$$

$$f_{p1} = f_{p0} + \frac{2(f_{pe} - f_{p0})x_1}{l_p} \quad (7)$$

It is assumed that the slope of σ_{p1} at $x = 0$ is zero [i.e., $\sigma'_{p1}(0) = 0$]. Then, the three second-order stress distributions, $\sigma_{p1}(0 \leq x \leq x_1)$, $\sigma_{p2}(x_1 \leq x \leq x_2)$, and $\sigma_{p3}(x_2 \leq x \leq l_p/2)$ can be determined using the following boundary conditions with f_{p0} , f_{p1} , and f_{p2} as determined from Eqs. (3) and (7):

$$\sigma_{p1}(0) = f_{p0}$$

$$\sigma'_{p1}(0) = 0$$

$$\sigma_{p2}(x_1) = \sigma_{p1}(x_1) = f_{p1}$$

$$\sigma'_{p2}(x_1) = \sigma'_{p1}(x_1)$$

$$\sigma_{p3}(x_2) = \sigma_{p2}(x_2) = f_{p2}$$

$$\sigma'_{p3}(x_2) = \sigma'_{p2}(x_2)$$

$$t_p \int_0^{x_1} \sigma_{p1} dx + t_p \int_{x_1}^{x_2} \sigma_{p2} dx + t_p \int_{x_2}^{l_p/2} \sigma_{p3} dx = \frac{P_i + G_p + G_a}{2} \quad (8)$$

Figs. 7(a) and 7(b) compare the estimated base panel top stress distributions with stress distributions determined using the finite element analysis results of a selected set of parametric walls for varying values of

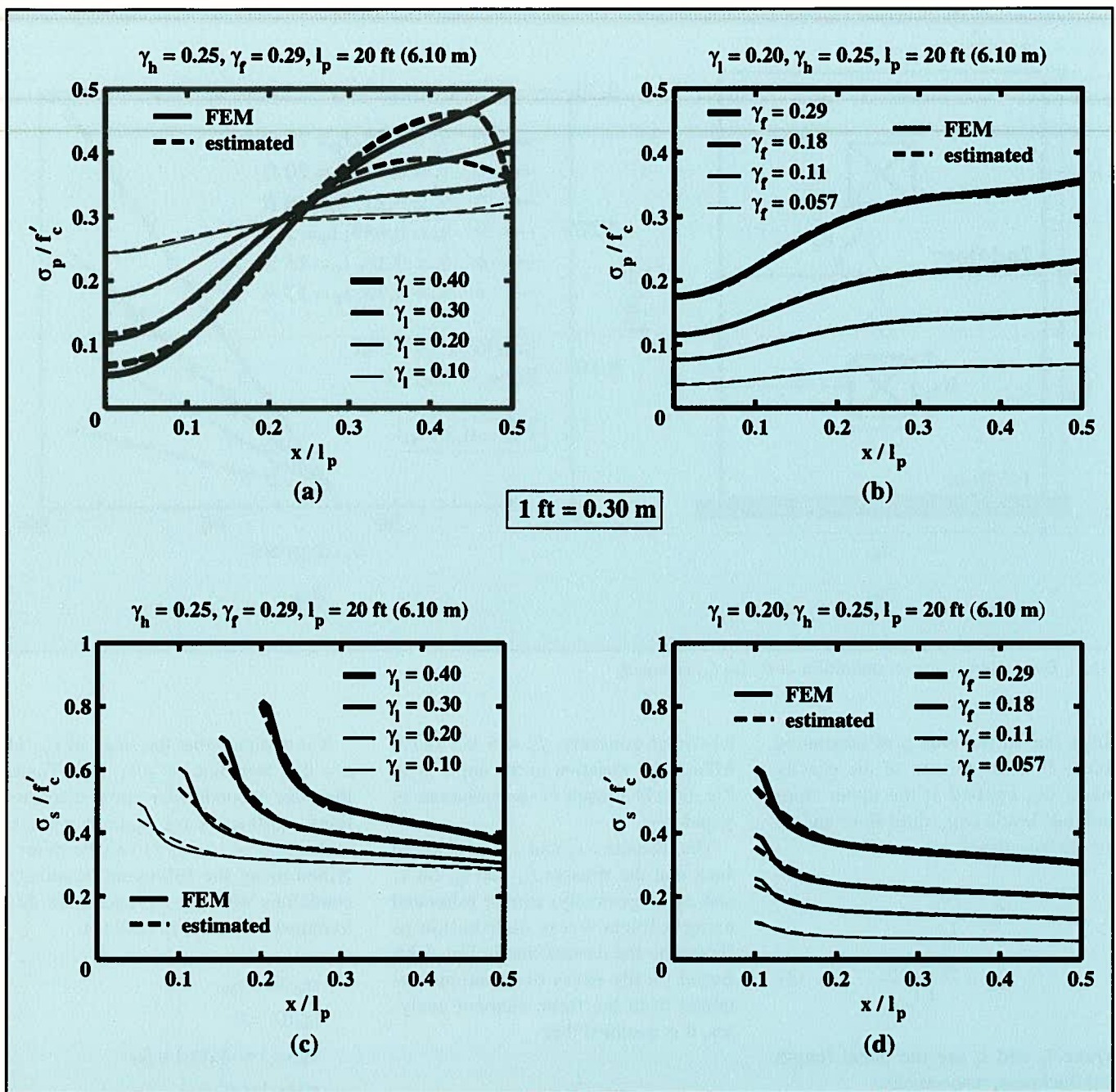


Fig. 7. Stress distributions: (a), (b) panel top stresses; (c), (d) side chord stresses.

γ_l [with $\gamma_h = 0.25$, $\gamma_f = 0.29$, $l_p = 20$ ft (6.10 m)] and γ_f [with $\gamma_l = 0.20$, $\gamma_h = 0.25$, $l_p = 20$ ft (6.10 m)], respectively. The stresses are normalized with respect to $f'_c = 6$ ksi (41.4 MPa).

The results in Figs. 7(a) and 7(b) indicate that the estimated stress distributions are close to the FEM distributions (i.e., the distributions obtained using the finite element model). For the cases of γ_l equal to 0.30 and 0.40 with $\gamma_h = 0.25$, $\gamma_f = 0.29$, and $l_p = 20$ ft (6.10 m) [Fig. 7(a)], which correspond to two of the longer openings in Wall

WH1M, the estimated stress distributions deviate from the FEM distributions near the end of the panels (i.e., near $x = l_p/2$). However, this deviation does not significantly affect the estimation of the required panel reinforcement since only a portion of the stress distribution over a distance of x_r from the panel centerline is used in the truss model as shown in Fig. 5(b).

Estimation of C_r and \bar{x}_p

The truss model in Fig. 5(b) uses the portion of the panel top stresses be-

tween $0 \leq x \leq x_r$, with a compressive stress resultant equal to C_r and a resultant location equal to \bar{x}_p . Based on the finite element analysis results, it is assumed that:

$$x_r = \frac{l_c}{2} + 0.3l_c \quad (9)$$

where l_c is the length of the side chord as shown in Fig. 5(a). Thus, C_r and \bar{x}_p can be determined by integrating the estimated panel top stress distribution from $x = 0$ to $x = x_r$, as:

$$C_r = t_p \left(\int_0^{x_1} \sigma_{p1} dx + \int_{x_1}^{x_r} \sigma_{p2} dx \right)$$

$$\bar{x}_p = t_p \frac{\int_0^{x_1} \sigma_{p1} x dx + \int_{x_1}^{x_r} \sigma_{p2} x dx}{C_r} \quad (10)$$

Note that $x_1 < x_r < x_2$; thus, both σ_{p1} and σ_{p2} need to be estimated to determine C_r and \bar{x}_p .

Estimation of Side Chord Stresses and \bar{x}_s

The compressive stress distribution at the top of the side chord is estimated as follows. The stress distribution from $x = l_p/2$ to $x = l_p/2$ is divided into two parts, σ_{s1} and σ_{s2} , between $l_p/2 \leq x \leq x_r$ and $x_r \leq x \leq l_p/2$, respectively [where x_r is given in Eq. (9)]. The compressive stress resultant for σ_{s1} is assumed to be equal to C_r and the compressive stress resultant for σ_{s2} is assumed to be equal to $(P_i + G_p + G_a)/2 - C_r$.

The stress f_{sr} at $x = x_r$ is estimated using a uniform stress distribution in the side chord as shown by the dashed line in Fig. 5(b) as:

$$f_{sr} = \frac{P_i + G_p + G_a}{2l_c t_p} \quad (11)$$

Then, the stress f_{se} at $x = l_p/2$ is determined assuming a linear stress distribution for σ_{s2} as:

$$f_{se} = \frac{P_i + G_p + G_a - 2C_r}{(l_p/2 - x_r) t_p} - f_{sr} \quad (12)$$

Finally, a second order stress distribution is assumed for σ_{s1} , which can be determined using the following boundary conditions:

$$\sigma_{s1}(x_r) = \sigma_{s2}(x_r) = f_{sr}$$

$$\sigma'_{s1}(x_r) = \sigma'_{s2}(x_r) = \frac{f_{sr} - f_{se}}{l_p/2 - x_r} \quad (13)$$

$$t_p \int_{\frac{l_p}{2}}^{x_r} \sigma_{s1} dx = C_r$$

After finding σ_{s1} , the location of the

stress resultant C_r at the top of the side chord, \bar{x}_s , can be determined as follows:

$$\bar{x}_s = \frac{t_p \int_{\frac{l_p}{2}}^{x_r} \sigma_{s1} x dx}{C_r} \quad (14)$$

Figs. 7(c) and 7(d) compare the estimated base panel side chord stress distributions with stress distributions determined using the finite element analysis results of a selected set of parametric walls for varying values of γ_l [with $\gamma_h = 0.25$, $\gamma_f = 0.29$, $l_p = 20$ ft (6.10 m)] and γ_f [with $\gamma_l = 0.20$, $\gamma_h = 0.25$, $l_p = 20$ ft (6.10 m)], respectively. The stresses are normalized with respect to $f'_c = 6$ ksi (41.4 MPa). The results indicate that the estimated stress distributions are close to the FEM distributions.

Placement of the Panel Reinforcement

The design approach described above can be used to determine the panel reinforcement needed to limit the size of cracks that can occur at an opening. The finite element analysis results indicate that the tensile stresses above and below the opening are similar. Thus, the reinforcement determined for the top of the opening can and should also be used at the bottom of the opening. It is recommended that:

- The welded wire fabric used in the panels be ignored, and
- A minimum reinforcement of two No. 5 bars [with an area $A_{min} = 0.61$ sq in. (394 mm²)] be used along the top and bottom edges of the opening.

The reinforcing bars should be placed as close to the top and bottom edges of the opening as possible (with adequate concrete cover and clear distances between the bars) on both faces of the panel. The reinforcement should be placed horizontally within the depth of the tension region, h_{tv} , above and below the opening [see Fig. 5(a)]. Based on the finite element analysis results, it may be assumed that:

$$h_{tv} = \gamma_l h_c \quad (15)$$

For the walls investigated in this study, the proposed design requirements can be met without using very large bars since the amount of reinforcement needed in the panels is not excessive, as shown later.

The reinforcing bars should be extended a sufficient distance on both sides of the middle of the opening to provide adequate length for the development of the steel strength. The tension regions at the top and bottom of the opening extend the entire length of the opening [see Fig. 4(a)]. Thus, the length of each bar should be greater than the opening length to provide sufficient embedment beyond the opening corners.

Design of the Upper Story Panels

The finite element analysis results of the parametric walls show that tensile stresses form along the top and bottom edges of the openings in the upper story panels, similar to the base panel. The magnitude of these tensile stresses is most significant in walls with large amounts of post-tensioning (e.g., $\gamma_f = 0.29$).

As an example, Figs. 8(a) and 8(b) show the maximum principal stress contours over the height of Wall WH1M [$\gamma_f = 0.29$ and $l_p = 20$ ft (6.10 m)] without and with openings ($\gamma_l = 0.40$ and $\gamma_h = 0.38$), respectively. The red-shaded areas indicate regions of the wall panels where the maximum principal stresses exceed $7.5\sqrt{f'_c}$ in tension and, thus, where cracking is expected to occur.

Fig. 8(b) shows that the size of the critical regions with tensile stresses larger than $7.5\sqrt{f'_c}$ decreases in the upper story panels. Several of the upper story panels in Fig. 8(b) do not have any regions with tensile stresses exceeding $7.5\sqrt{f'_c}$. However, the finite element analysis results show that significantly large (but less than $7.5\sqrt{f'_c}$) tensile stresses do form along the top and bottom edges of the openings in these panels and, thus, bonded mild steel reinforcement is recommended.

The proposed design approach can be used for the upper story panels similar to the design of the base panel described earlier. The only differences between the base panel and the upper

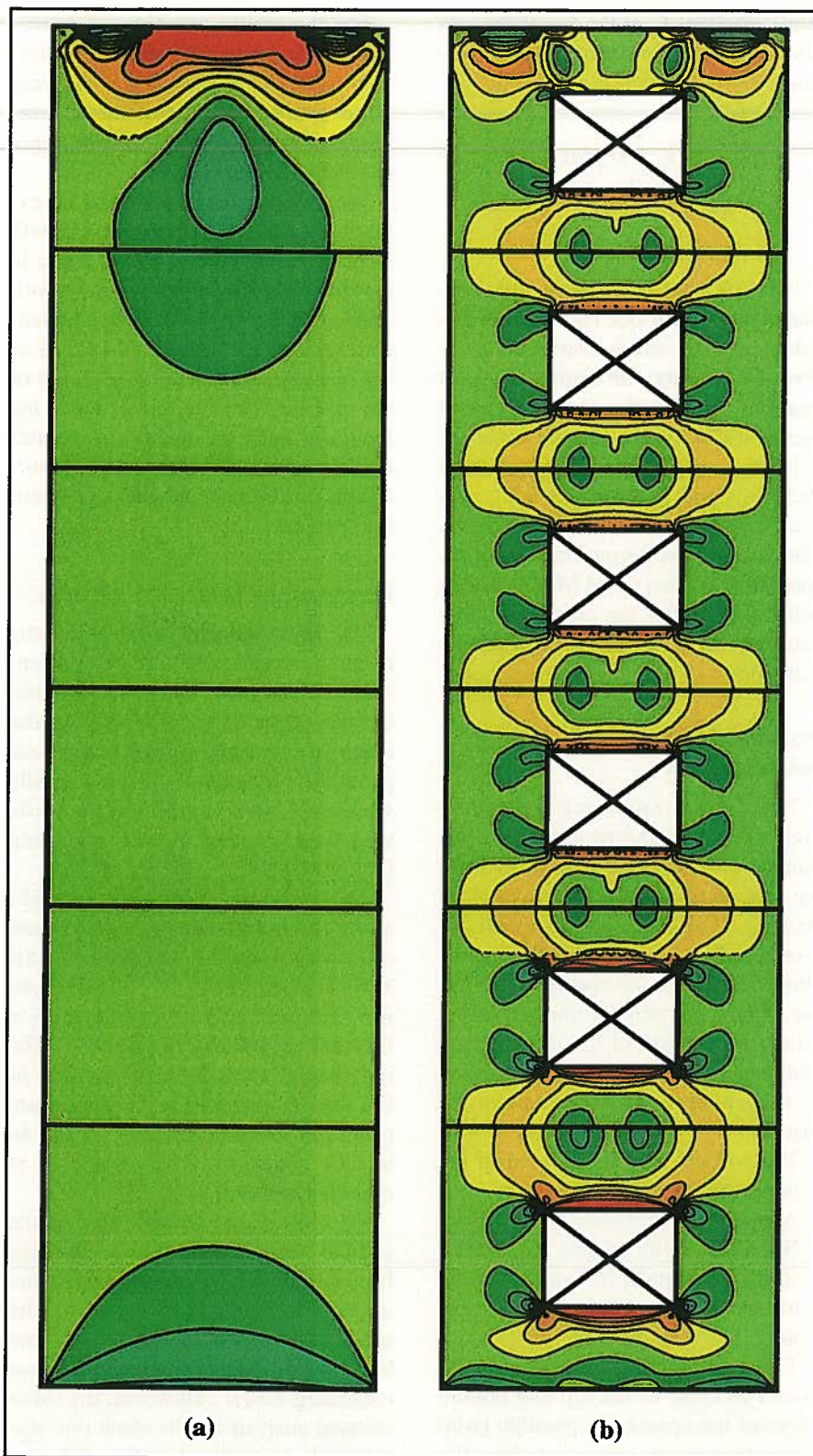


Fig. 8. Principal stress contours in Wall WH1M ($\gamma_f = 0.29$, $l_p = 20$ ft): (a) without openings; (b) with openings ($\gamma_l = 0.40$, $\gamma_h = 0.38$).

story panels for the design of the panel reinforcement are the amount of gravity load and, possibly, the panel height. Thus, the proposed design approach can be applied to the upper story panels by using the appropriate

panel height and the gravity loads acting on the panel.

As in the base panel, a minimum reinforcement of two No. 5 bars is recommended along the top and bottom edges of the openings in the upper

story panels. Note that the proposed design approach cannot be used for the roof panel where there is no panel above and concentrated post-tensioning anchor forces are applied. This paper does not address the design of the roof panel for the post-tensioning anchor forces.

For walls where the post-tensioning forces are significantly larger than the gravity loads, it is recommended that the reinforcement designed for the base panel be used in the upper story panels since the critical tensile stresses in the panels will be similar. For walls with little or no post-tensioning, it may be more economical to determine the reinforcement needed in each individual panel.

RESULTS OF STUDY

For each parametric wall, the required reinforcing steel area, A_v , above and below the opening in the base panel is predicted using the proposed design approach and compared with the steel area determined using the finite element model (referred to as the FEM steel area). To determine the FEM steel area, the tensile stresses above the opening were integrated over the height of the tension region, h_{rv} , and then divided by the assumed yield strength of the steel, f_y , of 60 ksi (414 MPa).

Note that even though the required steel area, A_v , for the walls investigated in this paper is determined based on the assumed yield strength of the steel, f_y , a more conservative allowable steel strength f_{all} equal to $0.5f_y$ is recommended for use in practice. Then, the required steel areas given below should be multiplied by 2.0.

Table 2 compares the predicted and FEM steel areas, A_v , for the base panels of the parametric walls normalized with respect to the horizontal chord area $h_c t_p$, resulting in the required reinforcement ratio, ρ_v , as:

$$\rho_v = \frac{A_v}{h_c t_p} \quad (16)$$

In Table 2, the values in bold correspond to the cases where the predicted reinforcement ratio is less than the FEM reinforcement ratio.

Table 2. Required reinforcement at top and bottom of opening.

γ_l	γ_h	$l_p = 20$ ft								$l_p = 15$ ft		$l_p = 12$ ft	
		$\gamma_f = 0.29$		$\gamma_f = 0.18$		$\gamma_f = 0.11$		$\gamma_f = 0.057$		$\gamma_f = 0.18$		$\gamma_f = 0.18$	
		ρ_v (percent) FEM	ρ_v (percent) Pred.										
0.10	0.13	0.11	0.11	—	—	—	—	0.021	0.021	—	—	—	—
0.20	0.13	0.20	0.22	—	—	—	—	0.041	0.046	—	—	—	—
0.30	0.13	0.28	0.32	0.18	0.21	0.12	0.14	0.058	0.069	0.17	0.18	0.15	0.16
0.40	0.13	0.34	0.40	—	—	—	—	0.071	0.092	—	—	—	—
0.10	0.25	0.12	0.12	0.076	0.078	0.049	0.051	0.023	0.024	0.070	0.066	0.062	0.055
0.20	0.25	0.22	0.23	0.14	0.15	0.092	0.10	0.044	0.049	0.12	0.12	0.11	0.10
0.30	0.25	0.28	0.32	0.18	0.21	0.12	0.14	0.059	0.071	0.18	0.19	0.17	0.17
0.40	0.25	0.31	0.37	0.21	0.25	0.14	0.17	0.070	0.091	0.22	0.24	0.22	0.23
0.10	0.38	0.13	0.14	—	—	—	—	0.026	0.028	—	—	—	—
0.20	0.38	0.22	0.24	—	—	—	—	0.046	0.052	—	—	—	—
0.30	0.38	0.26	0.29	0.17	0.19	0.11	0.13	0.058	0.070	0.18	0.19	0.18	0.18
0.40	0.38	0.26	0.30	—	—	—	—	0.066	0.085	—	—	—	—
avg(pred./FEM)		1.10		1.12		1.14		1.16		1.05		0.99	

Note: The ρ_v values should be multiplied by 2.0 if $f_{alt} = 0.5f_y$ is used in design.
 $\gamma_l = l_o/l_p$, $\gamma_h = h_o/h_p$, and $\gamma_f = f_{ci}/f'_c$, where $h_p = 16$ ft and $f'_c = 6.0$ ksi.
 1 ft = 0.3048 m, 1 ksi = 6.895 MPa.

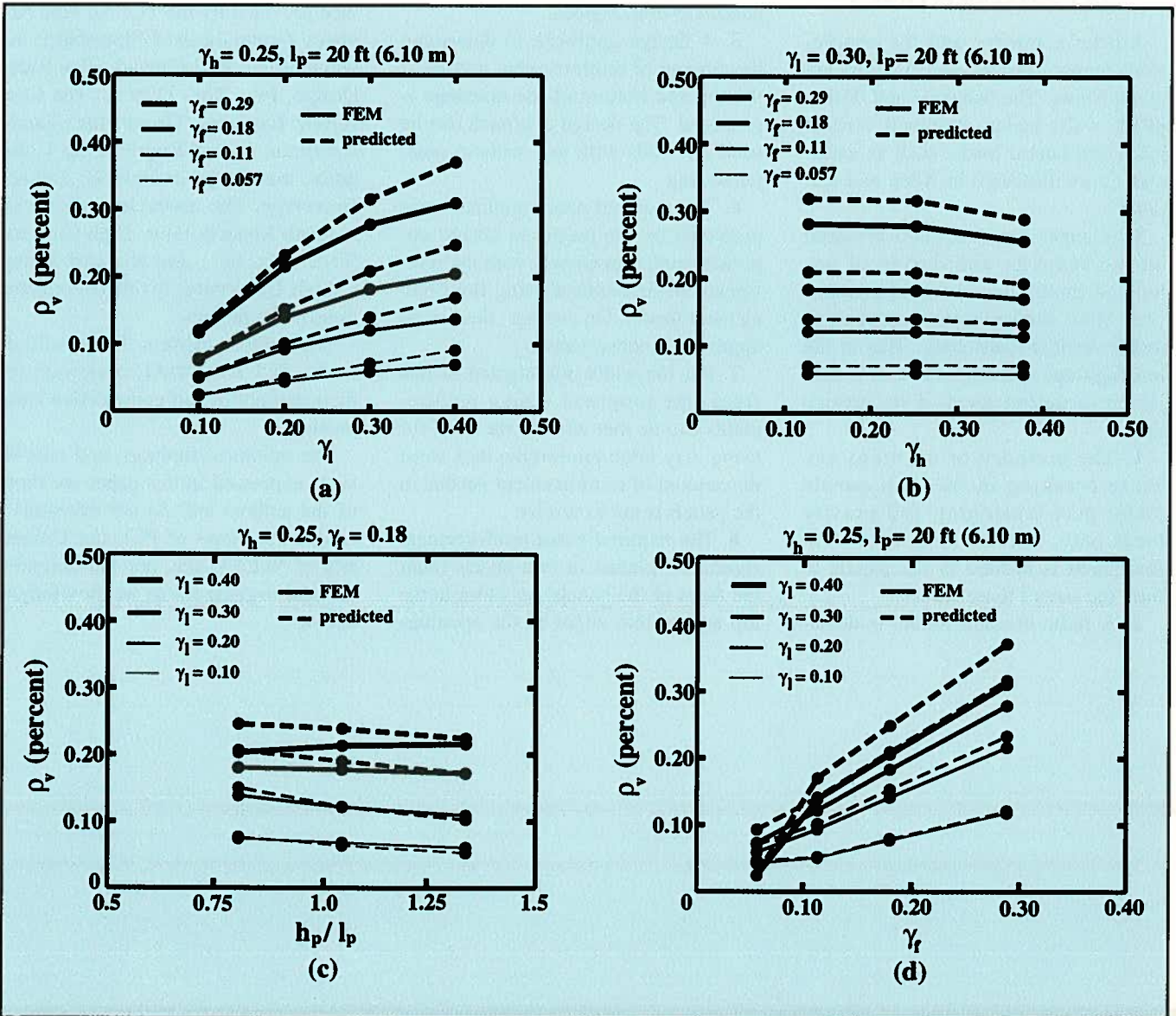


Fig. 9. Reinforcement ratio, ρ_v : (a) effect of γ_l ; (b) effect of γ_h ; (c) effect of h_p/l_p ; (d) effect of γ_f .

Selected results from the observed trends and comparisons based on the parametric analyses are given in Fig. 9, which shows the predicted and FEM reinforcement ratios for different values of γ_l , γ_h , l_p , and γ_f . The results indicate that the required reinforcement ratio, ρ_v , increases as γ_l increases and γ_f increases.

Table 2 shows the average of the predicted reinforcement ratios divided by the FEM reinforcement ratios for each combination of l_p and γ_f . The results indicate that the design approach, on average, provides a reasonably close and conservative [except for $l_p = 12$ ft (3.66 m)] estimate for the required panel reinforcement in the walls.

CONCLUSIONS AND RECOMMENDATIONS

A brief summary and the conclusions drawn from the investigation are given below. The behavior and design of the walls under combined vertical loads and lateral loads, such as earthquakes are discussed in Allen and Kurama.⁶

This paper has described research on the behavior and design of unbonded post-tensioned precast concrete walls with rectangular openings under vertical loads only. This is the loading stage that a typical wall is subjected to during most of its service life.

1. The presence of openings can cause cracking in the wall panels under post-tensioning and gravity loads only. Bonded mild steel reinforcement is needed in the panels to limit the size of these cracks.

2. A finite element model is devel-

oped to investigate the behavior and design of walls with openings. The finite element model is verified by comparing the maximum tensile stresses around the openings with available closed-form analytical solutions.

3. The finite element model is used to conduct a parametric investigation on the behavior and design of a series of walls. The parameters studied are the opening length, opening height, panel length, and initial stress in the concrete due to post-tensioning and gravity loads.

4. The parametric analyses show that the most critical regions in the wall panels under vertical loads are at the top and bottom of the openings. The tensile stresses above and below an opening are similar and, thus, similar amounts of reinforcement are needed in both regions.

5. A design approach to determine the amount of reinforcement needed at the top and bottom of the openings is proposed. The design approach can be used for walls with and without post-tensioning.

6. The required panel reinforcement predicted by the proposed design approach compares closely with the reinforcement determined using the finite element model. On average, the design approach is conservative.

7. For the walls investigated in this study, the proposed design requirements can be met without the need for using very large reinforcing bars since the amount of reinforcement needed in the panels is not excessive.

8. The required panel reinforcement should be placed in two layers (near the faces of the panels), as close to the top and bottom edges of the openings

as possible. The reinforcement should be placed horizontally within the tension region and should be extended a sufficient distance beyond the corners of the openings with adequate length to develop the steel strength.

ACKNOWLEDGMENTS

The research was funded by a PCI Daniel P. Jenny Research Fellowship and by the University of Notre Dame. The support of the Precast/Prestressed Concrete Institute and the University of Notre Dame is gratefully acknowledged.

The support of Paul Johal, PCI research director, and Helmuth Wilden, past chairman of the PCI Research and Development Committee, is gratefully acknowledged. The support and advice provided by the PCI Ad Hoc Advisory Group on the Fellowship is acknowledged: Ned Cleland, Blue Ridge Design, Inc.; Tom D'Arcy, The Consulting Engineers Group, Inc.; James Hoffman, Sturm Engineering Company; and Stephen Pessiki, Lehigh University. The researchers also wish to thank Kenneth Baur, High Concrete Structures, Inc., and Richard Sause, Lehigh University, for their contributions to the project.

The authors express their gratitude to the PCI JOURNAL reviewers for their thoughtful and constructive comments.

The opinions, findings, and conclusions expressed in this paper are those of the authors and do not necessarily reflect the views of PCI, the University of Notre Dame, nor the individuals and organizations acknowledged above.

REFERENCES

1. Kurama, Y., Pessiki, S., Sause, R., and Lu, L., "Seismic Behavior and Design of Unbonded Post-Tensioned Precast Concrete Walls," *PCI JOURNAL*, V. 44, No. 3, May-June 1999, pp. 72-89.
2. Kurama, Y., Sause, R., Pessiki, S., and Lu, L., "Lateral Load Behavior and Seismic Design of Unbonded Post-Tensioned Precast Concrete Walls," *ACI Structural Journal*, V. 96, No. 4, July-August 1999, pp. 622-632.
3. Kurama, Y., Pessiki, S., Sause, R., Lu, L., and El-Sheikh, M., "Analytical Modeling and Lateral Load Behavior of Unbonded Post-Tensioned Precast Concrete Walls," Research Report No. EQ-96-02, Department of Civil and Environmental Engineering, Lehigh University, Bethlehem, PA, November 1996, 191 pp.
4. Priestley, M., Sritharan, S., Conley, J., and Pampanin, S., "Preliminary Results and Conclusions From the PRESSS Five-Story Precast Concrete Test Building," *PCI JOURNAL*, V. 44, No. 6, November-December 1999, pp. 42-67.
5. Allen, M., and Kurama, Y., "Design of Rectangular Openings in Unbonded Post-Tensioned Precast Concrete Walls," Research Report No. NDSE-01-01, Department of Civil Engineering and Geological Sciences, University of Notre Dame, Notre Dame, IN, April 2001 (available for download at <http://www.nd.edu/~concrete>).
6. Allen, M., and Kurama, Y., "Design of Rectangular Openings in Precast Walls Under Combined Vertical and Lateral Loads." To be published in the March-April 2002 *PCI JOURNAL*.
7. Kurama, Y., "Simplified Seismic Design Approach for Friction-Damped Unbonded Post-Tensioned Precast Concrete Walls," *ACI Structural Journal*, V. 98, No. 5, September-October 2001, pp. 705-716.
8. Perez, F., "Lateral Load Behavior of Precast Concrete Walls with Ductile Vertical Joint Connectors," M.S. Thesis, Department of Civil and Environmental Engineering, Lehigh University, Bethlehem, PA, December 1998.
9. Hibbitt, Karlsson, and Sorenson, *ABAQUS User's Manual*, Hibbitt, Karlsson, & Sorenson, Inc., Version 5.8, 1998.
10. Mander, J., Priestley, M., and Park, R., "Theoretical Stress-Strain Model for Confined Concrete," *ASCE Journal of Structural Engineering*, V. 114, No. 8, August 1988, pp. 1804-1826.
11. Savin, G., *Stress Concentrations Around Holes*, Pergamon Press, New York, NY, 1961.

APPENDIX A — NOTATION

A_g = gross cross-sectional area of wall A_{min} = minimum area of mild reinforcing steel (two No. 5 bars) a_p = area of a post-tensioning bar a_{pj} = first coefficient for σ_{pj} A_v = area of required mild reinforcing steel b_{pj} = second coefficient for σ_{pj} c_{pj} = third coefficient for σ_{pj} C_r = compression stress resultant in truss model C_v = compression stress resultant in horizontal chord f_{all} = allowable strength of mild reinforcing steel f'_c = compressive strength of unconfined concrete f_{ci} = initial stress in concrete f_p = compression stress applied to panel f_{p0} = compression stress at top of panel at centerline f_{p1} = compression stress at top of panel at x_1 f_{p2} = compression stress at top of panel at x_2 f_{pa} = uniformly distributed stress transferred from panel above f_{pe} = compression stress at top of panel at edge (based on a linear stress distribution) f_{pi} = initial stress in post-tensioning steel f_{pp} = uniformly distributed stress due to gravity load applied at floor level above panel f_{pu} = ultimate strength of post-tensioning steel f_{py} = yield strength of post-tensioning steel f_{se} = compression stress in side chord at edge of panel f_{sr} = compression stress in side chord at x_r f_{tm} = maximum tension stress at top of opening f_y = yield strength of mild reinforcing steel G_a = sum of gravity loads applied at upper floor and roof levels G_b = total axial force in base panel due to gravity loads G_p = gravity load applied at floor level above panel h_c = height of horizontal top chord or bottom chord	h_o = height of opening h_p = height of panel h_{pu} = height of upper story panel h_w = height of wall l_c = length of side chord l_o = length of opening l_p = length of panel P_i = sum of initial forces in post-tensioning bars t_p = thickness of panel T_v = tension stress resultant at top of opening x = horizontal distance measured from centerline of panel x_1 = location where σ_{p1} changes to σ_{p2} x_2 = location where σ_{p2} changes to σ_{p3} \bar{x}_p = resultant location of C_r at top of panel x_r = distance over which stresses are integrated to determine C_r \bar{x}_s = resultant location of C_r at top of side chord γ_f = ratio of f_{ci} to f'_c γ_h = ratio of h_o to h_p γ_l = ratio of l_o to l_p θ_c = angle to determine f_{p0} (in degrees) θ_t = angle for truss model (in degrees) ρ_{sp} = volume of spiral reinforcing steel divided by volume of confined concrete core ρ_v = required mild steel reinforcement ratio σ_p = panel top stress distribution σ_{p1} = second order panel top stress distribution in Region 1 σ_{p2} = second order panel top stress distribution in Region 2 σ_{p3} = second order panel top stress distribution in Region 3 σ_{pj} = second order panel top stress distribution in Region j σ_s = side chord stress distribution σ_{s1} = second order side chord stress distribution in Region 1 σ_{s2} = first order side chord stress distribution in Region 2
---	---

APPENDIX B — DESIGN EXAMPLE

The following example demonstrates the implementation of the proposed design approach to determine the required panel reinforcement in a six-story wall with $l_p = 20$ ft (6.10 m), $\gamma_f = 0.18$, $\gamma_l = 0.30$, and $\gamma_h = 0.38$. The dimensions of the wall and the placement of the post-tensioning bars are shown in Fig. 2(b). The applied loads, wall and opening dimensions, and material properties are given below.

Data

Post-tensioning and gravity loads:

$$P_i = 2280 \text{ kips (10140 kN)}$$

$$G_p = 172 \text{ kips (765 kN) at the second floor level, 167 kips (743 kN) at the third through sixth floor levels, and 143 kips (636 kN) at the roof}$$

$$G_b = 172 + 4 \times 167 + 143 = 983 \text{ kips (4370 kN)}$$

Wall and panel dimensions:

$$l_p = 240 \text{ in. (6100 mm)}$$

$$h_p = 192 \text{ in. (4880 mm) for the base panel and 160 in. (4060 mm) for the upper story panels}$$

$$t_p = 12 \text{ in. (305 mm)}$$

Opening and chord dimensions:

$$l_o = 72 \text{ in. (1830 mm)}$$

$$l_c = (240 - 72)/2 = 84 \text{ in. (2130 mm)}$$

$$h_o = 72 \text{ in. (1830 mm)}$$

$$h_c = (192 - 72)/2 = 60 \text{ in. (1520 mm) for the base panel and } (160 - 72)/2 = 44 \text{ in. (1120 mm) for the upper story panels}$$

Material properties:

$$f'_c = 6 \text{ ksi (41.4 MPa)}$$

$$f_y = 60 \text{ ksi (414 MPa)}$$

Design Overview

The design of the base panel, which is the most critical panel, is presented below. The post-tensioning forces for the wall are significantly larger than the gravity loads. Thus, the reinforcement determined for the base panel will be used in the upper story panels as described at the end of the design example.

Estimation of Panel Top Stresses

In order to determine the amount of reinforcement required at the top and bottom of the opening in the base panel, it is necessary to solve Eq. (1) for T_v and A_v . The first step is to estimate the stresses at the top of the panel by using Eq. (2) for the regions $0 \leq x \leq x_1$ and $x_1 \leq x \leq x_2$, where x is measured from the centerline of the panel. Using Eq. (6):

$$x_1 = 72/2 = 36 \text{ in. (914 mm)}$$

$$x_2 = (2 \times 72 + 240)/4 = 96 \text{ in. (2440 mm)}$$

The stresses f_{p1} and f_{p2} (at x_1 and x_2 , respectively) are esti-

mated using a linear stress distribution as shown by the dashed line in Fig. 5(b). For the base panel,

$$G_p = 172 \text{ kips (765 kN)}$$

$$G_a = 4 \times 167 + 143 = 811 \text{ kips (3610 kN)}$$

Thus, f_{pp} and f_{pa} can be determined from Eq. (4) as:

$$f_{pp} = 172/(240 \times 12) = 0.0597 \text{ ksi (0.412 MPa)}$$

$$f_{pa} = (2280 + 811)/(240 \times 12) = 1.07 \text{ ksi (7.38 MPa)}$$

The angle θ_c is calculated using Eq. (5). For the base panel, $h_{pu} = 160$ in. (4060 mm) and, thus,

$$\theta_c = \tan^{-1}[(160 - 72)/72] = 50.7 \text{ degrees}$$

The stresses f_{pp} and f_{pa} , and the angle θ_c , are then used in Eq. (3):

$$f_{p0} = 1.07(50.7 - 40)/45 + 0.0597 = 0.315 \text{ ksi (2.17 MPa)}$$

The stresses f_{pe} , f_{p2} , and f_{p1} are determined using Eq. (7):

$$f_{pe} = 2(2280 + 172 + 811)/(240 \times 12) - 0.315 = 1.96 \text{ ksi (13.5 MPa)}$$

$$f_{p2} = 0.315 + 2 \times 96(1.96 - 0.315)/240 = 1.63 \text{ ksi (11.2 MPa)}$$

$$f_{p1} = 0.315 + 2 \times 36(1.96 - 0.315)/240 = 0.809 \text{ ksi (5.58 MPa)}$$

The stresses f_{p1} and f_{p2} are then used in Eq. (8) to determine the boundary conditions for the panel top stresses σ_{p1} and σ_{p2} as:

$$\sigma_{p1}(0) = 0.315 \text{ ksi (2.17 MPa)}$$

$$\sigma'_{p1}(0) = 0$$

$$\sigma_{p2}(36) = \sigma_{p1}(36) = 0.809 \text{ ksi (5.58 MPa)}$$

$$\sigma'_{p2}(36) = \sigma'_{p1}(36)$$

$$\sigma_{p2}(96) = 1.63 \text{ ksi (11.2 MPa)}$$

These boundary conditions can be used to determine the distributions for the panel top stresses σ_{p1} and σ_{p2} as:

$$\sigma_{p1} = (3.74 \times 10^{-4})x^2 + 0.315 \text{ (ksi)}$$

$$\sigma_{p2} = (-2.24 \times 10^{-4})x^2 + 0.0431x - 0.463 \text{ (ksi)}$$

Estimation of C_r and \bar{x}_p

The stress distributions σ_{p1} and σ_{p2} are then used to estimate C_r and \bar{x}_p based on Eqs. (9) and (10) as follows:

$$x_r = 72/2 + 0.3 \times 84 = 61.2 \text{ in. (1550 mm)}$$

$$C_r = 533 \text{ kips (2370 kN)}$$

$$\bar{x}_p = 38.7 \text{ in. (983 mm)}$$

Estimation of Side Chord Stresses and \bar{x}_s

After determining C_r and \bar{x}_p , the stresses at the top of the side chord can be estimated. The stress f_{sr} is found using Eq. (11):

$$f_{sr} = (2280 + 172 + 811)/(2 \times 84 \times 12) \\ = 1.62 \text{ ksi (11.2 MPa)}$$

The stress f_{se} is calculated using Eq. (12):

$$f_{se} = (2280 + 172 + 811 - 2 \times 533)/[(240/2 - 61.2)12] - 1.62 \\ = 1.49 \text{ ksi (10.3 MPa)}$$

The boundary conditions for σ_{s1} are determined using Eq. (13):

$$\sigma_{s1}(61.2) = \sigma_{s2}(61.2) = 1.49 \text{ ksi (10.3 MPa)} \\ \sigma'_{s1}(61.2) = \sigma'_{s2}(61.2) = (1.62 - 1.49)/(240/2 - 61.2) \\ = 0.00221$$

$$12 \int_{36}^{61.2} \sigma_{s1} dx = 533 \text{ kips (2370 kN)}$$

These boundary conditions are then used to solve for σ_{s1} :

$$\sigma_{s1} = (6.37 \times 10^{-4})x^2 - 0.0803x + 4.13 \text{ (ksi)}$$

From Eq. (14), \bar{x}_s can be calculated as:

$$\bar{x}_s = 48.0 \text{ in. (1220 mm)}$$

Estimation of T_v and A_v

The design tension stress resultant T_v , the required reinforcement area A_v , and the reinforcement ratio ρ_v in the base panel are estimated using Eqs. (1) and (16). In this design example, the required reinforcement area, A_v , is determined based on the steel yield strength, f_y . As described in the paper, a more conservative allowable steel strength, $f_{all} = 0.5f_y$, is recommended for use in practice. Then, the A_v and ρ_v values calculated below should be multiplied by 2.0.

$$T_v = 533(48.0 - 38.7)/60 = 82.6 \text{ kips (367 kN)}$$

$$A_v = 82.6/60 = 1.38 \text{ sq in. (890 mm}^2\text{)} > A_{min} = 0.61 \text{ sq in. (394 mm}^2\text{)} \\ \text{(OK)}$$

Thus,

$$\rho_v = 1.38 \times 100/(60 \times 12) \\ = 0.19 \text{ percent as shown in Table 2.}$$

Reinforcement Selection and Placement

The required reinforcement in the base panel is provided using 8 No. 4 bars [with an area of 1.57 sq in. (1013 mm²)]; four bars near each face of the panel, placed at both

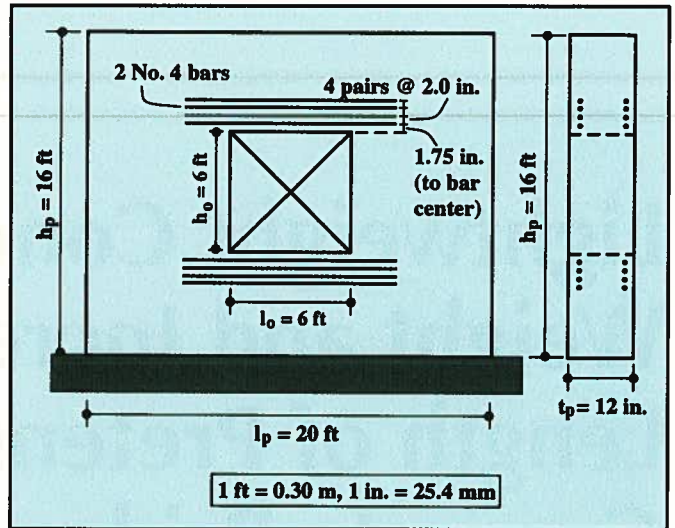


Fig. B1. Design example.

the top and the bottom of the opening as shown in Fig. B1. Based on Eq. (15), the bars should be placed within a distance of:

$$h_{nv} = 0.30 \times 60 = 18 \text{ in. (457 mm)}$$

from the opening top and bottom edges to ensure that the reinforcement is within the tension region.

Using a center-to-center spacing of 2.0 in. (50.8 mm) and allowing 1.5 in. (38.1 mm) of clear cover concrete to the first layer of bars, the reinforcement can be placed within 8.0 in. (203 mm) from the edges of the opening. The bars should be extended a sufficient distance past the opening corners with adequate length for the development of the steel strength.

Design of Upper Story Panels

As described earlier, the reinforcement ratio of $\rho_v = 0.19$ percent for the base panel is also used in the upper story panels. Since the height of the horizontal chord, h_c , in the upper story panels is less than the height of the chord in the base panel, a smaller reinforcement area may be used in the upper story panels as:

$$A_v = 0.19 \times 12 \times 44 / 100 \\ = 1.00 \text{ sq in. (645 mm}^2\text{)} > A_{min} = 0.61 \text{ sq in. (394 mm}^2\text{)} \\ \text{(OK)}$$

The design of the top (roof) panel for the post-tensioning anchor forces is not addressed in this example.